

Na₂Si₃O₇: an incommensurate structure with crenel-type modulation functions, refined from a twinned crystal

Hannes Krüger,^{a*} Volker
Kahlenberg^a and Karen Friese^b

^aInstitut für Mineralogie und Petrographie,
Leopold-Franzens-Universität, 6020 Innsbruck,
Austria, and ^bDepartamento Física Materia
Condensada, Universidad del País Vasco, Apdo
644, 48080 Bilbao, Spain

Correspondence e-mail:
hannes.krueger@uibk.ac.at

Received 20 January 2006
Accepted 22 February 2006

The structure of metastable, incommensurately modulated Na₂Si₃O₇ has been determined from single-crystal X-ray diffraction data. In contrast to previous investigations which stated that the compound crystallizes in an orthorhombic space group, this study shows that the compound is monoclinic with a pseudo-orthorhombic cell and is affected by twinning. The structure is described in the (3 + 1)-dimensional super-space. Crenel-type modulation functions are used to account for an aperiodic sequence of right- and left-handed *zweier* single chains of silicate tetrahedra. The modulation mainly affects one of the two symmetrically independent tetrahedral chains, which are connected to build up [Si₃O₇]²⁻ layers. Sodium cations are coordinated by five oxygen ligands and provide linkage between adjacent tetrahedral sheets. Distortions of the silicate tetrahedra and crystal chemical relationships of the title compound to sodium and lithium di- and metasilicates are discussed in detail.

1. Introduction

The Na₂O–SiO₂ system and the phase relationships between the crystalline and vitreous sodium silicates have been the subject of many investigations (Williamson & Glasser, 1965, 1966; Hoffmann & Scheel, 1969; Shahid & Glasser, 1971; Scherer & Uhlmann, 1975; Mogensen & Christensen, 1981; Neilson & Weinberg, 1984; Zaitsev *et al.*, 1999; Meshalkin & Kaplun, 2003). This activity is mainly due to the fact that these compounds are of considerable importance in material science: sodium silicates are the basic constituents in the synthesis of glasses and ceramics. However, crystalline phases such as Na₂Si₂O₅ have been studied because of their high ion-exchange capacity and selectivity (Wolf & Schwieger, 1979), as well as their two-dimensional sodium diffusion and conductivity (Heinemann & Frischat, 1990). A review of industrial uses with an emphasis on applications as builders in washing powders can be found in the article of Rieck (1996). From a crystal chemist's point of view it is interesting to note that the existence of several sodium silicates has been known for more than 40 years, although their crystal structures remained to be solved. For example, only very recently a detailed structural study of Na₆Si₈O₁₉ has been reported (Krüger *et al.*, 2005). An important reason for the problems with the structural characterizations can be definitely attributed to the fact that many of the SiO₂-rich phases reported in the literature are metastable compounds and consequently of low quality for X-ray diffraction. One of the phases belonging to this class of materials is sodium trisilicate, Na₂O·3SiO₂. Williamson & Glasser (1966) prepared single crystals of Na₂Si₃O₇ from the devitrification of glasses with > 67 mol% SiO₂ at temperatures of ~ 923 K and reported an orthorhombic *C*-centered

Table 1
Experimental details.

Crystal data	
Chemical formula	Na ₂ Si ₃ O ₇
<i>M_r</i>	242.2
Cell setting, superspace group	Monoclinic, <i>C2/c</i> (0 β 0) <i>s</i> 0
Temperature (K)	298
<i>a</i> , <i>b</i> , <i>c</i> (Å)	20.416 (6), 6.4987 (15), 4.9294 (19)
β (°)	90.26 (3)
Modulation wavevector	q = 0.562 (2) b *
<i>V</i> (Å ³)	654.0 (4)
<i>Z</i>	4
<i>D_x</i> (Mg m ⁻³)	2.459
Radiation type	Mo <i>K</i> α
No. of reflections for cell parameters	2604
θ range (°)	2–27.0
μ (mm ⁻¹)	0.85
Crystal form, color	Plate, colorless
Crystal size (mm)	0.28 × 0.1 × 0.03
Data collection	
Diffractometer	Stoe IPDS-II
Data collection method	Rotation method
Absorption correction	None
No. of measured, independent and observed reflections	4714, 1914, 1327
Criterion for observed reflections	<i>I</i> > 3 σ (<i>I</i>)
<i>R</i> _{int}	0.082
θ _{max} (°)	26.7
Range of <i>h</i> , <i>k</i> , <i>l</i>	–25 \Rightarrow <i>h</i> \Rightarrow 25 –8 \Rightarrow <i>k</i> \Rightarrow 8 –6 \Rightarrow <i>l</i> \Rightarrow 4
Refinement	
Refinement on	<i>F</i>
<i>R</i> [<i>F</i> ² > 2 σ (<i>F</i> ²)] (all, main, sat)	0.073, 0.053, 0.101
<i>wR</i> (<i>F</i> ²) (all, main, sat)	0.065, 0.051, 0.092
<i>S</i>	2.30
No. of reflections	1914
No. of parameters	157
Weighting scheme	Based on measured s.u.s., <i>w</i> = 1/[σ^2 (<i>F</i>) + 0.0001 <i>F</i> ²]
(Δ / σ) _{max}	<0.0001
$\Delta\rho$ _{max} , $\Delta\rho$ _{min} (e Å ⁻³)	1.07, –0.80

Computer programs used: *Stoe X-AREA* (Stoe & Cie GmbH, 2005), *JANA2000* (Petříček *et al.*, 2000); structural graphics were prepared using *DRAWxtl* (Finger *et al.*, 2005).

unit cell of *a* = 20.6, *b* = 6.50, *c* = 4.90 Å. A subsequent structural study of Jamieson (1967) on these crystals revealed that the diffraction pattern was much more complex, involving additional satellite reflections with non-integral indices. Focusing on the strong main reflections a preliminary structural model for Na₂Si₃O₇ was sketched in the space group *Cmc2*₁. However, due to an unacceptable final *R* index of ~ 0.18, in combination with extremely high atomic displacement parameters for some of the O atoms, no atomic coordinates were reported. On the other hand, Na₂Si₃O₇ can occur in a second modification. It is known that sodium trisilicate prepared from the careful dehydration of Na₂Si₃O₇·H₂O at 713 K adopts an interrupted framework structure with three- and four-connected [SiO₄] tetrahedra with a ratio of *Q*³:*Q*⁴ = 2:1 (Kahlenberg *et al.*, 2002). Furthermore, a high-pressure modification of Na₂Si₃O₇ has also been described (Fleet & Henderson, 1995) and crystallizes in a monoclinic framework structure containing diorthosilicate [Si₂O₇] groups as well as isolated [SiO₆] octahedra. A discussion on polymorphism of

[Si₃O₇] anions in layered silicates was published by Pushcharovsky & Belov (1978). The present investigation was designed to investigate the apparently modulated structure of Na₂Si₃O₇ in more detail and to clarify structural relationships with other known silicates.

2. Experimental details

Single crystals of Na₂Si₃O₇ were grown by isothermal aging of a glass of stoichiometric composition. The glass was prepared by mixing the analysis-grade chemicals Na₂CO₃ and SiO₂ (fine grained quartz) in a molar ratio of 1:3. The mixture was homogenized in an agate mortar and subsequently placed in a platinum crucible. The reagents were high-temperature treated at 1773 K for 1 h in a resistance-heated furnace, followed by quenching to room conditions. The glass obtained was used as the starting material for devitrification by static heat treatment at 873 K. Single crystals were found in samples heated for 48 h. They were generally of bad optical quality and their X-ray diffraction patterns were also of poor quality. In order to achieve crystals of better characteristics devitrification experiments at 873 K were performed for up to 34 d. Unfortunately, even after this long heat treatment the crystal quality did not significantly increase. Nevertheless, a platy-shaped crystal from this experiment was selected by optical criteria using a polarizing microscope and mounted on a glass fibre for single-crystal X-ray diffraction experiments. Further details of the data collection are summarized in Table 1. A reinvestigation of the same crystals 14 months after data collection (stored at room conditions) showed that the compound was not stable. The crystals decomposed to an amorphous material, which showed no significant diffraction intensities.

3. Refinement

As already pointed out by Jamieson (1967), the diffraction pattern of Na₂Si₃O₇ shows two types of reflections: the first type, strong Bragg reflections, can be indexed with a monoclinic *C*-centered lattice. The monoclinic angle is approximately 90°, implying high orthorhombic pseudosymmetry (see Table 1). The second type of reflections are generally weaker satellite reflections, which can be indexed with an incommensurate vector **q** of (0, β , 0) with β = 0.562 (2). The refinement of the cell parameters and the wavevector **q**, as well as the data reduction, was carried out using the software provided by Stoe & Cie GmbH (2005). The internal *R* value for the main reflections in the Laue group 12/*m*1 is 0.06, whereas *R*_{int} for the other settings (2/*m*11, 112/*m*), as well as for 2/*m*2/*m*2/*m* is ~ 0.14–0.16. The analysis of systematic absent reflections points to *Cc* or *C2/c* as possible space groups of the average structure. In fact, the structure could be solved in *C2/c* using direct methods (Altomare *et al.*, 1997) and was consecutively refined to a weighted *R* value of 0.32. The orthorhombic pseudosymmetry of the lattice suggested additional twinning. The difference of 0.26° between the monoclinic β angle and 90° should lead to a splitting of the

reflections with higher indices (h or l), if twinning is present. In reconstructed sections of the reciprocal space the reflections with higher l indices show an elongation along the a^* direction, suggesting a mirror plane perpendicular to the a axis as the twin element. The theoretical distance between the split diffraction spots (for the highest observed index $l = 6$) is $\sim 0.011 \text{ \AA}^{-1}$, alternatively 0.23, given in units of the index h . Owing to the small distances, the diffraction spots were not separated during the integration, leading to completely overlapped reflections. In fact, the refinement could be significantly improved ($wR = 0.18$) by introducing one of the additional orthorhombic symmetry elements as the twin operator (we chose the mirror plane perpendicular to the a axis). The twin volume fraction of individual (II) obtained in the final refinement is 0.330 (3). The introduction of anisotropic displacement parameters for all atoms led to a final wR value of 0.07 for the average structure.

For the satellite reflections an additional extinction rule for reflections $0k0m$ with $m \neq 2n$ is observed, suggesting the superspace symmetry element $\frac{2}{s}$. The only $(3 + 1)$ -dimensional superspace group in compliance with this condition is $C2/c(0\beta 0)s0$, which is an alternative setting of the superspace group $B2/b(00\gamma)s0$ (No. 15.3), as listed in Janssen *et al.* (1995). By choosing the \mathbf{q} vector within the first Brillouin zone [$\mathbf{q} = (0, 1 - \beta, 0)$, *i.e.* assigning the satellites to the main reflections extinct by the C lattice], the equivalent superspace group $X2/c(0\beta 0)s0$ with a centering vector of $(\frac{1}{2}, \frac{1}{2}, 0, \frac{1}{2})$ could be used. In order to conform to the cell chosen by Jamieson (1967), we decided to use the description in $C2/c(0\beta 0)s0$.

The refinement of the modulated structure was carried out using first-order satellite reflections only, as the average $I/\sigma(I)$ ratio of the second-order satellites was less than 1.4.

To describe the four-dimensional structure two crenel functions were employed (Petříček *et al.*, 1995) to define the occupational modulation of the atoms Si2 and O3. These atoms correspond to split-atom positions in the three-dimensional average structure, where two distinct orientations of one $[\text{SiO}_4]$ tetrahedra are realized. In the four-dimensional description the two split-atom positions of the ‘crenel atoms’

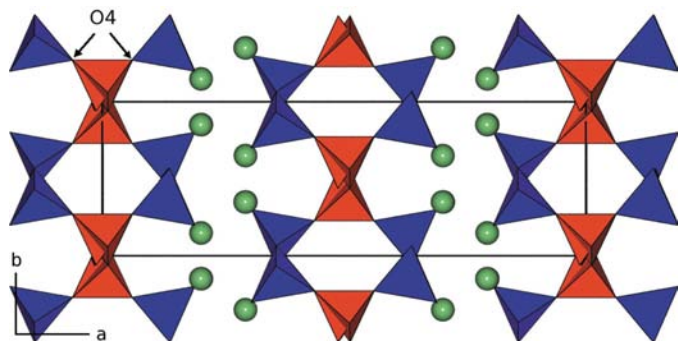


Figure 1
The layers viewed parallel to the direction of the chain. The lighter polyhedra represent the disordered central chain, the darker ones the outer chains. Spheres depict Na atoms.

Si2 and O3, respectively, are linked by the superspace symmetry element $\frac{2}{s}$ and are phase-shifted by $\tau = \frac{1}{2}$. To ensure that for all physical space sections only the atoms belonging to one of the two alternative tetrahedral positions are present, the phases of Si2 and O3 have to be restricted according to the following equation

$$t_4^0(\text{O3}) = t_4^0(\text{Si2}).$$

For the same reason, the widths of the crenel functions, expressed *via* the parameter Δ , also have to be set to be equal. Since these parameters did not refine to values significantly different from 0.5, they were fixed at this value. Values of Δ differing from 0.5 would lead to physically unacceptable situations: values larger than 0.5 would cause the existence of cells with two fully occupied sites, whereas $\Delta < 0.5$ would leave some cells unoccupied.

The only positional parameter of the ‘crenel atoms’, which was refined additionally with a harmonic modulation function was x_1 of Si2. Other positional modulations could only be refined by introducing an orthogonalization procedure (Petříček *et al.*, 1995) for the atoms Si2 and O3, respectively. Without the orthogonalization extremely large correlations between the coordinates of the atoms and the displacive modulation functions occurred. However, the refinement of more positional waves for Si2 and O3 did not significantly improve the refinement. Therefore, the orthogonalization method was not included in the final model.

For the remaining atoms all positional parameters, as well as anisotropic displacement parameters, were refined with first-order harmonic modulation functions.

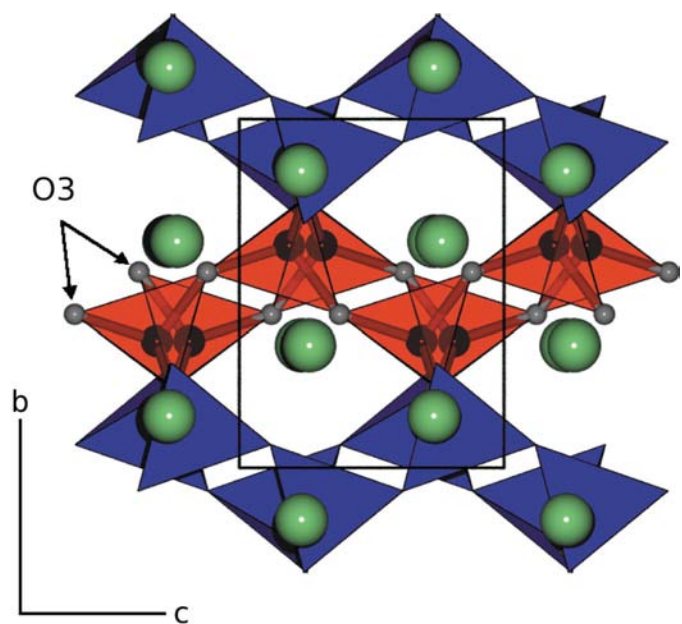


Figure 2
View parallel to the stacking direction of the sheets. Two distinct positions of the disordered central chain (transparent) are represented. Black spheres represent Si2 atoms, large light-coloured spheres Na atoms. One layer in the x range of 0.2–0.8 is shown.

4. Structure and modulations

As already shown by Jamieson (1967), $\text{Na}_2\text{Si}_3\text{O}_7$ is composed of layers of the composition $[\text{Si}_3\text{O}_7]^{2-}$, which are arranged parallel to the bc plane and stacked along the a direction (Fig. 1). Between the layers sodium cations are located to compensate for the charge. Each layer is built up by two independent tetrahedral chains running along c . The periodicity of these chains is two, therefore, they are called *zweier* single chains (Liebau, 1985). The silicate tetrahedra of the central chain (light-coloured in the figures) is Q^4 connected (*via* all four corners), while the outer chain (dark-coloured in the figures) has a lower connectedness of three. Each individual chain comprises only one symmetrically independent tetrahedra.

As can be seen in Fig. 2 the Q^4 chain is disordered in the average structure. The O4 atom connecting to the outer chains is fixed at one position, but the central silicon (Si2) and the O atom connecting along the chain direction (O3) occupy two positions with occupancy factors of 0.5. To show the distinct positions of the Si2 atom the central chain in Fig. 2 is kept transparent. The two resulting orientations of the central chain are enantiomorphs and can be arbitrarily called left- (L) and right-oriented (R).

The crenel modulation functions describing the positions of the Si2 and O3 atoms in the modulated structure are indicated in the the $x_3 - x_4$ sections (Figs. 3 and 4, respectively) of the electron density maps, as obtained from the the final refinement.

The two corresponding orientations of the tetrahedra are periodically alternating in the (3 + 1)-dimensional structure, whereas in three-dimensional physical space an aperiodic sequence of these two orientations is present within one layer. A similar incommensurately modulated sequence of tetrahedral chains was recently described by Krüger & Kahlenberg (2005) in the Brownmillerite-type compound $\text{Ca}_2\text{Fe}_2\text{O}_5$ at high temperatures. In the structure presented here, the basic sequence of the orientation of the central chain in physical space is alternating. After seven or eight alternations, RR or

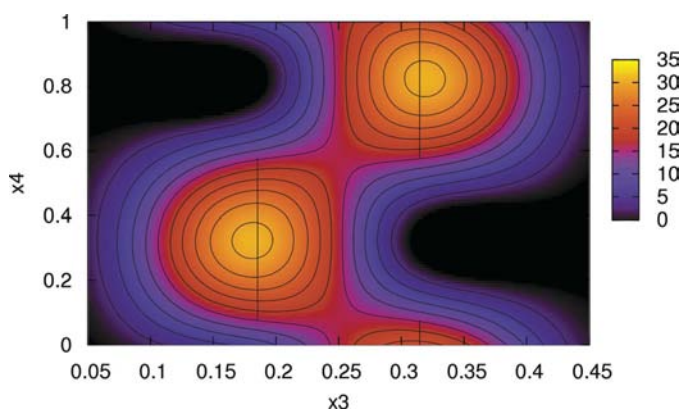


Figure 3

The crenel modulation function of the Si2 atom. $x_3 - x_4$ map, intersecting the four-dimensional F_{obs} Fourier synthesis at $x_1 = 0$, $x_2 = 0.136$. Contour lines from 3 to 30 $\text{e} \text{Å}^{-3}$ in intervals of 3 $\text{e} \text{Å}^{-3}$. The map is summed up in x_1 and x_2 over the range 0.5 Å .

LL pairs of equally oriented chains follow. A fragment of such a sequence could be: R-L-R-L-R-R-L-R-L-R-L-R-L-R-L-R-L-R-L-R-L-R-L. A two-dimensional physical space section (at $t = 0$) of the four-dimensional F_{obs} map intersecting at

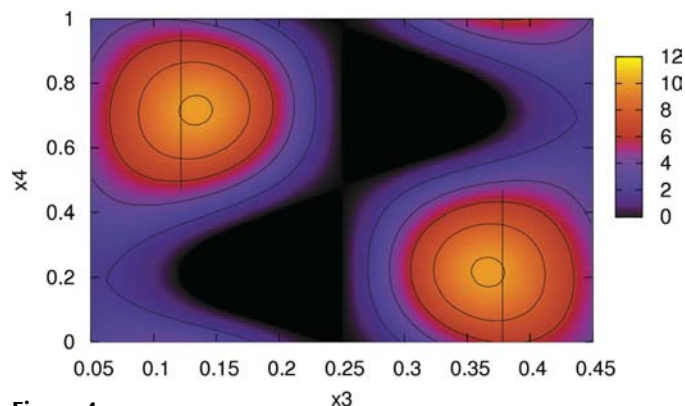


Figure 4

The crenel modulation function of the O3 atom. $x_3 - x_4$ map, intersecting the four-dimensional F_{obs} Fourier synthesis at $x_1 = 0$, $x_2 = -0.0607$. Contour lines from 2 to 10 $\text{e} \text{Å}^{-3}$ in intervals of 2 $\text{e} \text{Å}^{-3}$. The map is summed up in x_1 and x_2 over the range 0.5 Å .

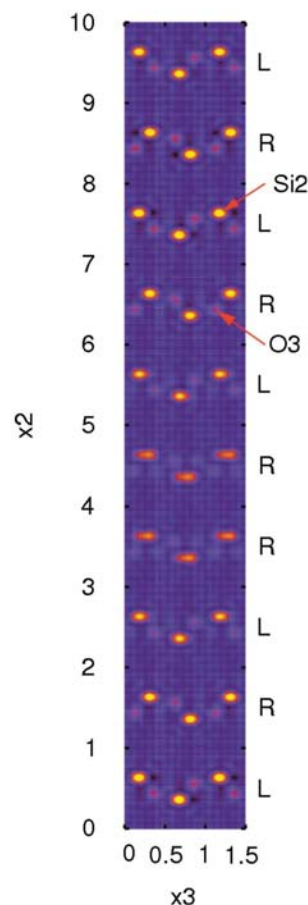


Figure 5

Physical space map ($x_2 - x_3$) at $t = 0$, $x_1 = 0.25$, calculated from four-dimensional F_{obs} Fourier synthesis. Incommensurately modulated sequence of right- (R) and left-handed (L) tetrahedral chains can be seen. The positions of Si2 and O3 are indicated.

$x_1 = 0.25$ (see Fig. 5) exhibits such a sequence of chains within one layer. This section cuts the central chains of one layer almost exactly at the coordinates of Si2 and O3. RR or LL pairs require the physical space section to cut the internal dimension close to the ‘jumps’ in the crenel functions. Due to a partial overlapping of the electron densities in these areas, the second orientation of the chain can be seen (although weaker) in the t map at $3 < x_2 < 5$.

The distances from Si2 to the tetrahedrally coordinating O atoms are shown in Fig. 6, for the t range 0–0.5 (corresponding to the width of the crenel function). The curves show the modulated distances, the constant lines of the same colour show the unmodulated distances between the atoms. For the two O4 atoms the unmodulated distances are quite short: 1.548 (4) and 1.566 (4) Å for O4 (x, y, z) and O4 ($-x, y, \frac{1}{2} - z$), respectively. The averaged distances as obtained from the modulated structure show larger values of 1.594 (7) and 1.589 (8) Å. Consequently, the modulation

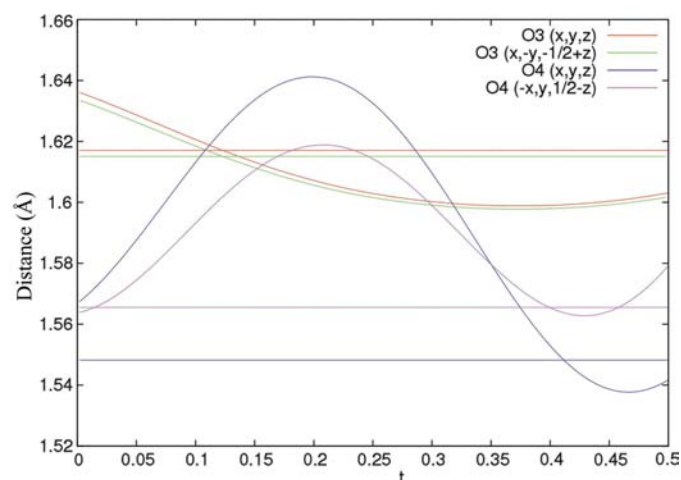


Figure 6
Modulated and unmodulated Si2–O distances.

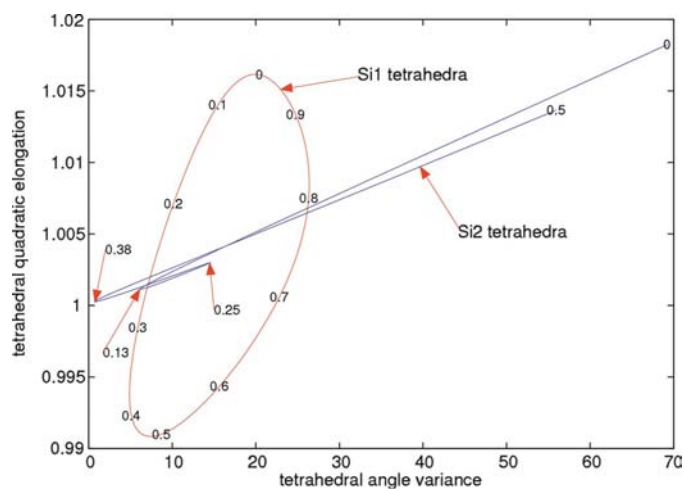


Figure 7
Distortion of Si1 and Si2 tetrahedra. Mean quadratic elongation plotted versus tetrahedral angle variance. Numbers next to the curves represent t values.

relaxes the Si2 tetrahedra (hereafter called T2). This effect can also be seen in the bond-valence sum (Brown & Altermatt, 1985) of Si2, the unmodulated value of which is 4.45 (10), yet the value averaged over the modulated structure is 4.28 (10).

The mean quadratic elongation ($\langle \lambda_{tet} \rangle$) and the tetrahedral angle variance $\sigma_{\theta(tet)}^2$, as defined by Robinson *et al.* (1971), were calculated as a function of t for the coordination tetrahedra of both Si atoms using *Mathematica* (Wolfram Research Inc., 2003). The t -dependent values of Si–O and O–O distances as well as O–Si–O angles were exported from Jana’s Graph-tool (plots of the O–O distances and O–Si2–O angles can be found in the supplementary material¹) and subsequently imported in *Mathematica* as interpolated functions. The volume of the tetrahedra was evaluated using the Cayley–Menger determinant (Weissenstein *et al.*, 2006).

The distortion diagram (Fig. 7) was obtained by plotting the mean tetrahedral quadratic elongation versus tetrahedral angle variance. T2 shows high distortions for t close to 0 and 0.5, which correspond to the limits of one continuous interval of the crenel functions. The plot exhibits a high linear correlation between $\langle \lambda_{T2} \rangle$ and $\sigma_{\theta(T2)}^2$, as found by Robinson *et al.* (1971) for a large number of rock-forming silicates. This is understandable if the fact that the displacive modulations affecting the T2 tetrahedra in this case are fairly simple is taken into account, and although all three fractional coordinates of O4 are affected by displacive modulation, O3 has no positional modulation at all and only one fractional coordinate (x_1) of Si2 is modulated.

The other tetrahedra (around Si1, hereafter called T1), which are only affected by displacive modulation, also show a relaxation of the bond-valence sum owing to the modulation. The unmodulated bond-valence sum is 4.14 (10); the average value for the modulated structure is 4.07 (10). A corresponding t -dependent plot can be found in the supplementary material. Si1 exhibits one short non-bridging bond to O2 [average 1.575 (7) Å]. Strong modulated distances are those to O1 ($\frac{1}{2} - x, \frac{1}{2} - y, -z$) and O1 ($\frac{1}{2} - x, \frac{1}{2} + y, \frac{1}{2} - z$), which show fluctuations from 1.603 (8)–1.723 (8) and 1.583 (7)–1.665 (7) Å, respectively. The bond distance of more than 1.72 Å seems to be quite large, but a plot of all distances regarding Si1 (Fig. 8) shows that the maximum (at $t \simeq 0$) in the Si1–O1 ($\frac{1}{2} - x, \frac{1}{2} - y, -z$) bond distance has to compensate for the other bonds, which exhibit minima at the same t . The fifth curve in Fig. 8 (denoted by l_0) represents the Si–O distance of an ideal tetrahedron of the same volume. This distance is used as a reference value in the calculation of the mean quadratic elongation. In the t interval between 0.28 and 0.69 the $\langle \lambda_{T1} \rangle$ parameter of T1 becomes smaller than one, which is caused by the minimum of three bond lengths in this interval. The maximum of the tetrahedral angle variance is 26.4 at $t \simeq 0.81$. The distortion plot of T1 exhibits an ‘egg-shaped’ outline and does not show any linear correlation between $\langle \lambda_{T1} \rangle$ and $\sigma_{\theta(T1)}^2$. All the atoms (of T1) involved are

¹ Supplementary data for this paper are available from the IUCr electronic archives (Reference: SN5035). Services for accessing these data are described at the back of the journal.

modulated in all directions, therefore, the O—O distances and O—Tl—O angle functions are represented by higher-order harmonic functions and do not show correlations.

A look at the environment of the Na atom reveals a fivefold coordination by oxygen. All coordinating O atoms belong to the outer tetrahedral chains (*i.e.* chains limiting the tetrahedral layer). Four of the O atoms form part of one tetrahedral layer, a fifth (O2) connects to a neighbouring layer (Fig. 9). The coordination polyhedra can be described as a trigonal bipyramid, where, in general, the equatorial coordinating O atoms are located at shorter distances than the axial O atoms. The variation of bond distances as observed in the modulated structures is given in Fig. 9. The extrema of the bond-valence sum of the Na atom are 0.94 (8) and 1.09 (8), and the average value is 1.01 (8). Additional *t*-dependent plots of the Na—O

distances and the bond-valence sum can be found in the supplementary material.

5. Discussion

A structural comparison of $\text{Na}_2\text{Si}_3\text{O}_7$ with sodium metasilicate Na_2SiO_3 (McDonald & Cruickshank, 1967) and sodium disilicate $\alpha\text{-Na}_2\text{Si}_2\text{O}_5$ (Pant & Cruickshank, 1968) was already realized by Jamieson (1967). The main results are the increasing condensation of the chains (with increasing SiO_2 content), as well as the fact that the coordination of the Na atoms remains essentially the same in the different compounds (*cf.* Fig. 3 in Jamieson, 1967).

Until now, only three other compounds, which may possibly exhibit a similar $[\text{Si}_3\text{O}_7]^{2-}$ silicate layer, have been discovered: $\text{Na}_2\text{Cu}(\text{Si}_3\text{O}_7)_2 \cdot 5\text{H}_2\text{O}$, a hydrated compound derived by acid leaching ($\text{H}_2\text{Si}_3\text{O}_7$), and $\text{Li}_2\text{Si}_3\text{O}_7$. For the sodium copper silicate an orthorhombic cell is given, determined by single-crystal diffraction: $a = 25.542$ (18), $b = 13.065$ (10), $c = 9.877$ (8) Å (Hubert *et al.*, 1977). The second compound was investigated by IR spectroscopy and powder diffraction techniques, and was considered to be of the same structural type, although the authors did not give any cell parameters (Guth *et al.*, 1977). By inspecting the cell of the copper compound it is obvious that the doubling of the *c* parameter (relative to the cell of $\text{Na}_2\text{Si}_3\text{O}_7$) would cause a doubling of the chain periodicity from two to four. The doubling of the *b* lattice parameter, on the other hand, could be evidence for a well ordered alternating sequence of L and R chains in the layer.

The third compound, $\text{Li}_2\text{Si}_3\text{O}_7$, was first described by West & Glasser (1970) and later studied by Morozova *et al.* (1972) and Kalinina *et al.* (1975). West & Glasser (1970) postulated a structure, similar to $\text{Na}_2\text{Si}_3\text{O}_7$, without giving further structural details. A detailed structural study on this compound is currently under progress in our laboratory.

Examples of the effect of substituting lithium for sodium can be seen in the di- and metasilicates. For lithium disilicate, for example, two modifications are known: a stable form described by Liebau (1961) and a metastable one (Smith *et al.*, 1990). Both structures contain tetrahedrally coordinated lithium located between the disilicate layers, whereas the configuration and arrangement of the strongly folded layers is different (see Figs. 1a and b in Smith *et al.*, 1990). In $\alpha\text{-Na}_2\text{Si}_2\text{O}_5$ (Pant & Cruickshank, 1968), the silicate layers are basically the same as in the metastable lithium disilicate. The coordination of the sodium anions is fivefold, as in $\text{Na}_2\text{Si}_3\text{O}_7$.

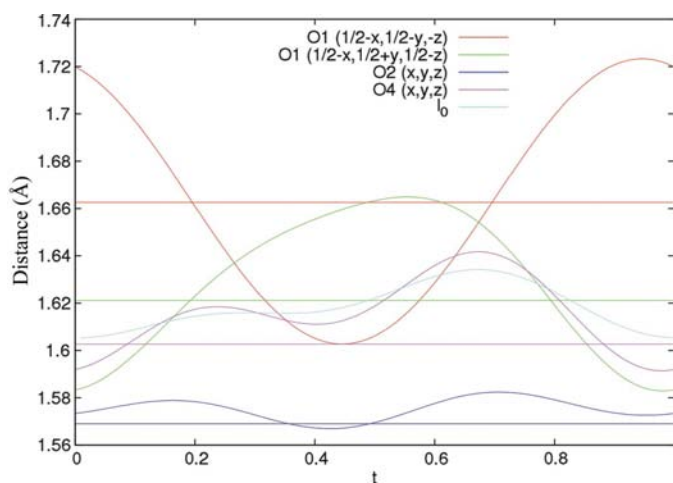


Figure 8
Modulated and unmodulated Si1—O distances.

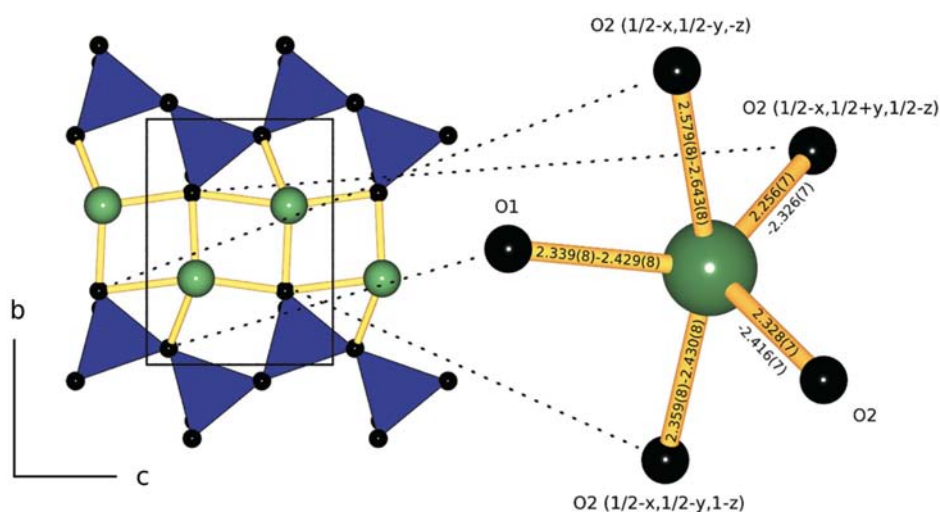


Figure 9
The coordination scheme of the Na atom in the average structure. The two outer tetrahedral chains (blue) belong to the closest neighbouring layer. One of the coordinating O atoms (O2) belongs to the next $[\text{Si}_3\text{O}_7]$ layer. Distances corresponding to the modulated structure are shown.

In the metasilicates the differences in the anion coordination are comparable: sodium is fivefold coordinated in Na_2SiO_3 (McDonald & Cruickshank, 1967), while lithium is tetrahedrally coordinated in Li_2SiO_3 (Hesse, 1977). The orientation of the tetrahedral chains is the same in both compounds. Investigations of West (1976) in the $\text{Na}_{2-x}\text{SiO}_3$ – Li_xSiO_3 system revealed a limited solid solubility. Samples with $x = 1$ showed a sixfold supercell along **a**. Further studies carried out by West (1977) confirmed the existence of a modulated structure. Later a detailed transmission electron microscopy study on the incommensurate phase in the range $0.86 \leq x \leq 1.02$ was carried out by Withers *et al.* (1989), who chose the same setting as Hesse (1977) for Li_2SiO_3 (*Cmc2₁*). According to the observed reflection conditions for the satellite reflections they proposed the superspace group *Cmc2₁(0 β 0)*s*0* [which is another setting of *A2₁ma(00 γ)0*s*0*, as listed as No. 36.8 in Janssen *et al.*, 1995]. Interestingly, the orientation of the modulation wavevector is essentially the same as in modulated $\text{Na}_2\text{Si}_3\text{O}_7$, *i.e.* both perpendicular to the direction of the chains and to the stacking direction of the layers (in metasilicates defined by layers of Li or Na). Furthermore, the intrinsic phase shift $\tau = \frac{1}{2}$ is common to both phases. Withers *et al.* (1989) suggest an antiphase relationship of the Li and Na occupation of symmetry-related sites. More detailed comparison of these two modulated structures requires a complete superspace-embedded structural model for the sodium–lithium metasilicate, which is not available at the moment. Future investigations should also concentrate on the question of solid solubility in the systems $\text{Na}_2\text{Si}_3\text{O}_7$ – $\text{Li}_2\text{Si}_3\text{O}_7$ and $\text{Na}_2\text{Si}_2\text{O}_5$ – $\text{Li}_2\text{Si}_2\text{O}_5$, respectively, and the corresponding structural consequences.

This work was supported by the *Acciones Integradas*, a bilateral agreement of the *Academic Cooperation and Mobility Unit* (ÖAD – Project No. 10/2005), the Spanish *Ministerio de Ciencia y Tecnología* and the *Gobierno Vasco*. The authors are very grateful to Václav Petříček for his continuous support with JANA2000, as well as to the referees for some valuable comments.

References

Altomare, A., Burla, M. C., Camalli, M., Cascarano, G., Giacovazzo, C., Guagliardi, A., Moliterni, A. G. G., Polidori, G. & Spagna, R. (1997). *SIR97*. Bari, Rome, Italy.
 Brown, I. D. & Altermatt, D. (1985). *Acta Cryst.* **B41**, 244–247.
 Finger, L., Kroeker, M. & Toby, B. (2005). *DRAWxtl*, Version 5.1; <http://www.lwfinger.net/drawxtl>.
 Fleet, M. E. & Henderson, G. S. (1995). *Phys. Chem. Miner.* **22**, 383–386.
 Guth, J.-L., Hubert, Y., Jordan, D., Kalt, A., Perati, B. & Wey, R. (1977). *C. R. Acad. Sci. D Nat.* **285**, 1367–1370.

Heinemann, I. & Frischat, G. (1990). *J. Am. Ceram. Soc.* **73**, 3712–3714.
 Hesse, K.-F. (1977). *Acta Cryst.* **B33**, 901–902.
 Hoffmann, W. & Scheel, H. (1969). *Z. Kristallogr.* **129**, 396–404.
 Hubert, Y., Jordan, D., Guth, J.-L. & Kalt, A. (1977). *C. R. Acad. Sci. D Nat.* **284**, 329–332.
 Jamieson, P. B. (1967). *Nature*, **214**, 794–796.
 Janssen, T., Janner, A., Looijenga-Vos, A. & de Wolff, P. M. (1995). *International Tables for Crystallography*, Vol. C, ch. 9.8. Dordrecht: Kluwer Academic Publishers.
 Kahlenberg, V., Marler, B., Muñoz Acevedo, J. C. & Patarin, J. (2002). *Solid State Sci.* **4**, 1285–1292.
 Kalinina, A. M., Maslenikov, A. V. & Filipovich, V. N. (1975). *Fiz. Khim. Stekla*, **1**, 144–149.
 Krüger, H. & Kahlenberg, V. (2005). *Acta Cryst.* **B61**, 656–662.
 Krüger, H., Kahlenberg, V. & Kaindl, R. (2005). *Solid State Sci.* **7**, 1390–1396.
 Liebau, F. (1961). *Acta Cryst.* **14**, 389–395.
 Liebau, F. (1985). *Structural Chemistry of Silicates – Structure, Bonding, and Classification*. Berlin: Springer-Verlag.
 McDonald, W. S. & Cruickshank, D. W. J. (1967). *Acta Cryst.* **22**, 37–43.
 Meshalkin, A. & Kaplun, A. (2003). *Russ. J. Inorg. Chem.* **48**, 1567–1569.
 Mogensen, G. & Christensen, N. H. (1981). *Phys. Chem. Glasses*, **22**, 17–22.
 Morozova, I. N., Gutkina, N. G. & Shmatok, L. K. (1972). *Prikl. Yad. Spektrosk.* **17**, 177.
 Neilson, G. F. & Weinberg, M. C. (1984). *J. Non-Cryst. Solids*, **63**, 365–374.
 Pant, A. K. & Cruickshank, D. W. J. (1968). *Acta Cryst.* **B24**, 13–19.
 Petříček, V., Dušek, M. & Palatinus, L. (2000). *JANA2000*. Institute of Physics, Praha, Czech Republic.
 Petříček, V., van der Lee, A. & Evain, M. (1995). *Acta Cryst.* **A51**, 529–535.
 Pushcharovsky, D. Y. & Belov, N. V. (1978). *Kristallografiya*, **23**, 756–763.
 Rieck, H. (1996). *Nachr. Chem. Tech. Lab.* **44**, 699–704.
 Robinson, K., Gibbs, G. V. & Ribbe, P. H. (1971). *Science*, **172**, 567–570.
 Scherer, G. & Uhlmann, D. (1975). *J. Cryst. Growth*, **29**, 12–18.
 Shahid, K. & Glasser, F. (1971). *Phys. Chem. Glasses*, **12**, 50–57.
 Smith, R. I., Howie, R. A. & West, A. R. (1990). *Acta Cryst.* **C46**, 363–365.
 Stoe & Cie GmbH (2005). *X-AREA*. Darmstadt, Germany.
 Weissenstein, E. W. *et al.* (2006). *From MathWorld – A Wolfram Web Resource*. <http://mathworld.wolfram.com/Cayley-MengerDeterminant.html>.
 West, A. R. (1976). *J. Am. Ceram. Soc.* **59**, 118–121.
 West, A. R. (1977). *Acta Cryst.* **A33**, 408–411.
 West, A. R. & Glasser, F. P. (1970). *Mater. Res. Bull.* **5**, 837–842.
 Williamson, J. & Glasser, F. P. (1965). *Science*, **148**, 1589–1591.
 Williamson, J. & Glasser, F. P. (1966). *Phys. Chem. Glasses*, **7**, 127–138.
 Withers, R. L., Thompson, J. G. & Hyde, B. G. (1989). *Acta Cryst.* **B45**, 136–141.
 Wolf, F. & Schwieger, W. (1979). *Z. Anorg. Allg. Chem.* **457**, 224–228.
 Wolfram Research, Inc. (2003). *Mathematica 5.0*. Champaign, Illinois, USA.
 Zaitsev, A. I., Shelkova, N. E., Lyakishev, N. P. & Mogutnov, B. M. (1999). *Phys. Chem. Chem. Phys.* **1**, 1899–1907.